Feasibility Study and Optimal Design of an Experimental Bench for Identification of Liquid Thermal Diffusivity

Laetitia Perez and Laurent Autrique

***Abstract*—Expertise of innovative materials by nondestructive techniques is a key goal in process engineering development. In this context, if identification of thermal diffusivity of liquid is a crucial requirement to develop a reliable mathematical model of knowledge, it is essential to propose a complete and valid methodology. Based on the analysis of thermal wave propagation (generated by a periodic excitation), an experimentation is developed in order to avoid the implementation of a pyroelectric sensor required in usual photopyroelectric techniques. The proposed approach is investigated in a trilayer system. Theoretical aspects of the identification of thermal parameters in the frequency domain are presented. A feasibility study is discussed in order to justify this approach for liquids. A sensitivity analysis is implemented in a particular case to provide an optimal experimental bench. Finally, experimental results for several liquids are presented and discussed.**

***Index Terms*—Frequency domain, nondestructive technique, optimal design, parametric identification, phase lag analysis.**

I. Introduction

In THE FIELD of thermal engineering, implementation of identification methods based on the analysis of thermal wave propagation (periodically generated by a heater device) presents various attractions [1]–[4]. These are illustrated by many applications and can include, for example, identification of thermal conductivity tensor of orthotropic materials [5] or that of thermal diffusivity of fibbers embedded in matrices [6]. Finally, in [7], several experimental devices based on periodic methods allowing investigations from micrometer scale to decimeter scale are presented.

In the specific framework of liquid thermal expertise using frequency domain approach, literature is less abundant than that for investigations of solid materials. The greatest number of related references is devoted to photopyroelectric methods (PPEMs) using different configurations. Such approaches have been used to obtain with great accuracy and sensibility thermal diffusivity in liquid samples. Considering the past decade, one can refer to the following studies. In [8], an application of PPEM at very low frequencies for thermal characterization of organosilane compounds is investigated. In [9], an original sample's thickness scan has been performed in order to identify thermal diffusivity of well-known liquids as well as water–alcohol mixtures. Vegetable oil thermal diffusivity has been identified in [10] using a new liquid-state design of the thermal wave resonator cavity (TWRC). Experimental TWRC setup for fluid thermophysical property measurements has been developed in [11] with a specific focus on 1-D and 3-D model comparisons. Photopyroelectric thickness scanning method is proposed in [12] for liquid thermal diffusivity identification (silicon oil). In [13], simultaneous determination of thermal effusivity and conductivity has been successfully carried out for several liquids in small quantity (water, paraffin oil, ethanol, and choline) using a self-calibrating approach. Last, a methodology using more than three layers has been recently reported in [14] and seems quite attractive in PPEM context.

One of the major difficulties in the thermal characterization of liquids lies in the sample setting and its geometry. In the following, an experimental approach is proposed in order to avoid the use of a pyroelectric layer such as lithium tantalate ($LiTaO_3$), polyvinylidene fluoride, or lead zirconate titanate (PZT, $PbZr_{0.3}Ti_{0.7}O_3$) films. Thus, an ordinary cell can be considered, and the induced experimental simplicity is quite attractive in the framework of specific liquids that are potentially sources of biological hazards or used in medical context. In fact, characterization of thermal properties of biological fluids must be regarded with the utmost attention given the disparities in the literature. For example, the thermal conductivity of the blood may vary between 0.49 and 0.75 $[W \cdot m^{-1} \cdot K^{-1}]$ according to the authors [15]–[19]. If the temperature rise in the skin induced by a burn or by a medical procedure (treatment of tumors by lasers, for example) has to be predicted using numerical models, the ignorance of the thermal conductivity of blood can be insurmountable. This key role has been pointed out in the prediction of skin burn induced by laser occurrence in [20] and [21].

In this paper, the feasibility aspects and the optimal design are discussed in order to define an experimental configuration allowing the identification of the considered thermophysical parameter using an unsophisticated cell. This paper is organized as follows. Section II is dedicated to the mathematical model proposed in order to estimate both phase and modulus of thermal wave in a 3-D geometry. In Section III, feasibility study is proposed. Then, an optimal configuration is determined

Manuscript received December 5, 2011; revised February 2, 2012; accepted March 3, 2012. Date of publication April 27, 2012; date of current version September 14, 2012. The Associate Editor coordinating the review process for this paper was Dr. Kurt Barbe.

L. Perez is with the Laboratoire de Thermocinétique de Nantes, LTN, UMR 6607, Ecole polytechnique de l'Université de Nantes, 44306 Nantes Cedex 3, France (e-mail: laetitia.perez@univ-nantes.fr).

L. Autrique is with the Laboratoire d'Ingénierie des Systèmes Automatisés, LISA-ISTIA, Université d'Angers, 49000 Angers, France (e-mail: Laurent.autrique@univ-angers.fr).

Color versions of one or more of the figures in this paper are available online at http://ieeexplore.ieee.org.

Digital Object Identifier 10.1109/TIM.2012.2193697

in Section IV in order to fulfill identification requirements. In Section VI, experimental device is presented, and several results are shown in order to discuss about the validation of the proposed approach. Then, several concluding remarks and outlooks are drawn up.

II. Modeling in the Frequency Domain

Let us consider the following notations: $\Omega \in \mathbb{R}^3$ is the space domain, $X = (x, y, z) \in \Omega$ is the space variable, and $t \in T$ is the time variable. The periodic heat flux on the surface $\Gamma \subset \partial\Omega$ boundary of Ω is expressed in the form

$$\phi(X,t) = \phi_0(X)F(t) \tag{1}$$

where ϕ_0 is the heat flux amplitude $(\mathrm{W}\cdot\mathrm{m}^{-2})$, $F(t) = a_0 + \sum_{n=1}^{\infty} b_n \cos(n\omega t - c_n)$, and ω is the pulsation $(\mathrm{rad}\cdot\mathrm{s}^{-1})$. Considering the initial temperature in the domain equal to the ambient temperature, evolution of temperature rise $\theta(X,t)$ in Ω is described by the following system of partial differential equations:

$$\begin{cases} C\frac{\partial\theta(X,t)}{\partial t} - \lambda\Delta\theta(X,t) = 0 & \forall (X,t) \in \Omega \times T \\ -\lambda\frac{\partial\theta(X,t)}{\partial\vec{n}} = h\theta X,t) - \phi(X,t) & \forall (X,t) \in \Gamma \times T \\ -\lambda\frac{\partial\theta(X,t)}{\partial\vec{n}} = h\theta(X,t) & \forall (X,t) \in \left(\frac{\partial\Omega}{\Gamma}\right) \times T \\ \theta(X, t=0) = 0 & \forall X \in \Omega \end{cases} \tag{2}$$

where C is the volumetric heat capacity $(\mathrm{J}\cdot\mathrm{m}^{-3}\cdot\mathrm{K}^{-1})$, λ is the thermal conductivity $(\mathrm{W}\cdot\mathrm{m}^{-1}\cdot\mathrm{K}^{-1})$, $\vec{n}$ is the normal vector exterior to the boundary $\partial\Omega$ of Ω, and h is the convective heat transfer coefficient $(\mathrm{W}\cdot\mathrm{m}^{-2}\cdot\mathrm{K}^{-1})$. Since the heat flux is periodic, temperature variations in Ω will be periodic as well. Considering that the steady state is obtained, the notion of complex temperature $\tilde{\theta}(X)$ can be used. Thus, a new system of partial differential equations is considered

$$\begin{cases} j\omega C\tilde{\theta}(X) - \lambda\Delta\tilde{\theta}(X) = 0 & \forall X \in \Omega \\ -\lambda\frac{\partial\tilde{\theta}(X)}{\partial\vec{n}} = h\tilde{\theta}(X) - \tilde{\Phi}(X) & \forall X \in \Gamma \\ -\lambda\frac{\partial\tilde{\theta}(X)}{\partial\vec{n}} = h\tilde{\theta}(X) & \forall X \in \left(\frac{\partial\Omega}{\Gamma}\right) \end{cases} \tag{3}$$

where $\tilde{\Phi}(X) = \phi_0(X)b_1$. The solution of the system (3) leads to determine at each point of the domain the modulus $M(X) = |\tilde{\theta}(X)|$ (amplitude) and the phase lag $\varphi(X) = \arg(\tilde{\theta}(X))$ (delay) of the heat wave resulting from the fundamental harmonic of the input signal $\phi(X,t)$. It is important to notice that system (3) becomes time independent which greatly reduces the computational time. From the numerical point of view, finite-element method is implemented using Comsol order to solve system (3). This is illustrated hereinafter for the following configuration: The domain Ω is a 0.1-m side square stainless steel thin plate and 2.10^{-3} m thick. The thermal excitation produced by a periodic heat flux is centered on its lower face. Let us consider that this flux excitation has a homogeneous "top hat" space distribution of radius $R = 2.10^{-3}$ m and that excitation frequency is $f = (\omega/2\pi) = 1$ Hz. The thermal stainless steel conductivity is $\lambda_{\mathrm{steel}} = 44.5\ [\mathrm{W}\cdot\mathrm{m}^{-1}\cdot\mathrm{K}^{-1}]$, the volumetric heat capacity is $C_{\mathrm{steel}} = 3.7\ 10^6\ [\mathrm{J}\cdot\mathrm{m}^{-3}\cdot\mathrm{K}^{-1}]$, and the convective heat transfer coefficient is $h = 10\ [\mathrm{W}\cdot\mathrm{m}^{-2}\cdot\mathrm{K}^{-1}]$. It is obvious that the amplitude of temperature oscillations depends on heating flux parameters which are quite difficult to quantify. Thus, if these parameters are not well known and controlled, any identification based on modulus observation is impossible. However, the phase lag does not depend on the heating flux amplitude but on excitation frequency. Thus, it appears as the relevant data for identification purposes. In Fig. 1, the phase lag between a point of the upper face and the center of the upper face versus the distance is plotted.

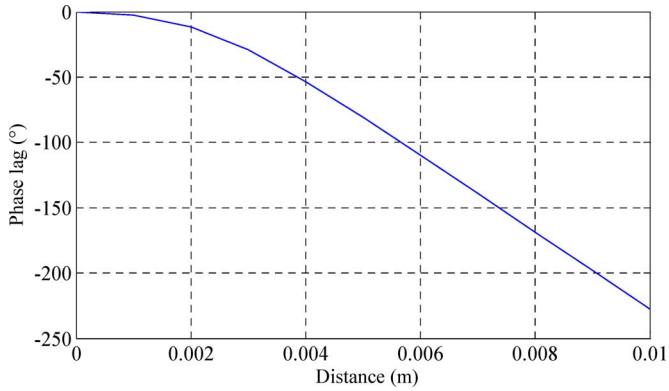

Fig. 1. Simulated phase lag.

It is well known that the phase lag observations are used to characterize materials and, in particular, their thermal diffusivity $\alpha = (\lambda/C)\ [\mathrm{m}^2\cdot\mathrm{s}^{-1}]$. Then, the following system is considered:

$$\begin{cases} -\Delta\tilde{\theta}(X) = -j\frac{\omega}{\alpha}\tilde{\theta}(X) & \forall X \in \Omega \\ -\frac{\partial\tilde{\theta}(X)}{\partial\vec{n}} = \frac{1}{\lambda}\left(h\tilde{\theta}(X) - \tilde{\Phi}(X)\right) & \forall X \in \Gamma \\ -\frac{\partial\tilde{\theta}(X)}{\partial\vec{n}} = \frac{h}{\lambda}\tilde{\theta}(X) & \forall X \in \left(\frac{\partial\Omega}{\Gamma}\right). \end{cases} \tag{4}$$

In the case of a liquid, the proposed approach is to keep the unknown liquid between two plates of reference materials (thermal properties of reference material have to be accurately known). At the fluid–solid interface (inside Ω), conditions of continuity in heat flux and temperature are assumed to be satisfied. In the following paragraph, the considered design options are be discussed.

III. Feasibility Study

In order to accurately identify the thermal diffusivity, it is essential to correctly take into account the thermal wave propagation in the trilayer material (reference + liquid + reference). Then, it is necessary to introduce the concept of diffusion length $\mu = \sqrt{\alpha/\pi f}$ [m]. In thermal sciences, it is commonly accepted that, at a distance of up to 3 μ, at least 95% of the thermal wave has disappeared. It means that the signal is too weak to remain informative. Then, several approaches can be implemented, and the following options have to be considered.

1) Transmission or reflection: Considering transmission, observable measurements and excitation are performed on opposite faces of the plane sample. In some situations where the opposite side of the sample is not accessible to measurement, observations have to be obtained on the same sample side (such methodology is called reflection).

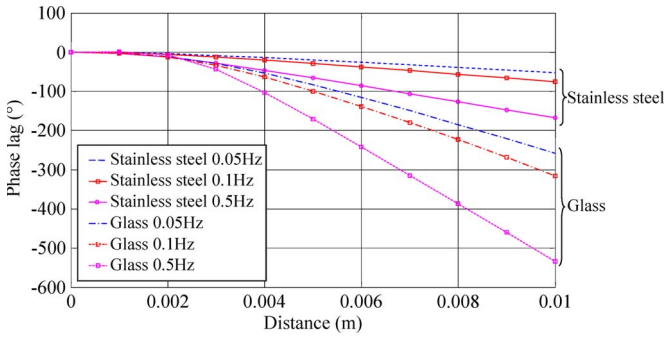

Fig. 2. Simulated phase lag in transmission for a stainless steel sample and a glass sample at different frequencies considering a spatial scanning.

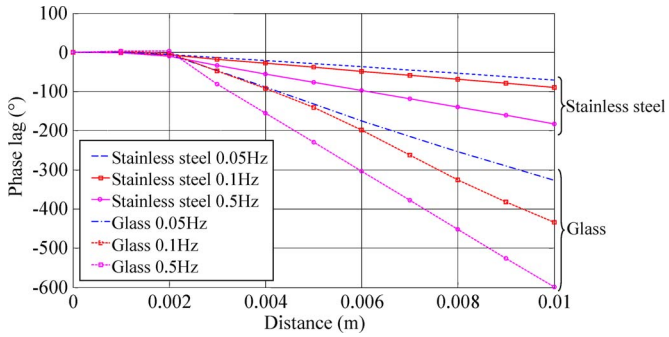

Fig. 3. Simulated phase lag in reflection for a stainless steel sample and a glass sample at different frequencies considering a spatial scanning.

2) Spatial scanning or frequency scanning: The phase lag of the thermal wave can be plotted versus the distance to the excitation at constant frequency; it is called spatial scanning. If observations are performed for a fixed point but for various frequencies, it is called frequency scanning.

Two distinct classes of material are considered for the reference material constituted the cell: thermal insulator or thermal conductor. One material of both classes will be tested: a glass cell or a stainless steel cell. Moreover, a mix cell (one glass layer and one steel layer) will be investigated.

A. Spatial Scanning: Transmission or Reflection

Let us consider that the liquid within the cell is water: $\lambda_{\text{water}} = 0.6$ [W · m^{-1} · K^{-1}]; $C_{\text{water}} = 4.2\ 10^6$ [J · m^{-3} · K^{-1}]. The reference material (cell) is an $e_{\text{ref}} = 5\ 10^{-4}$ [m] thin sample, while the thickness of the liquid is $e_{\text{water}} = 10^{-3}$ [m]. In the following figures, the phase lag in transmission and the phase lag in reflection are plotted for different frequencies: $f = 0.05$ [Hz], $f = 0.1$ [Hz], and $f = 0.5$ [Hz] versus the distance from the center of the excitation (spatial distribution of the periodic heat flux has been applied homogeneously on an $r = 2.10^{-3}$ [m] radius disk).

For a mix cell (one glass layer and one steel layer), two cases are studied for transmission analysis: case A for the heating flux applied on the steel layer while observations are performed on the glass layer; case B for the heating flux applied on the glass layer while observations are performed on the steel layer. Corresponding results are shown in Fig. 4. It is shown that cases A and B are similar and that phase lag magnitude can be compared with those obtained with steel cell (see Fig. 2).

For a mix cell (one glass layer and one steel layer), two cases are studied for reflection analysis: case C for the heating flux applied on the steel layer; case D for the heating flux applied on the glass layer. Corresponding results are shown in Fig. 5. It is shown that the results obtained in case C are similar to those obtained with steel cell (see Fig. 3). If the heating flux is applied on the glass face of the mix cell (case D), effect of the opposite steel face has to be taken into account since phase lag amplitude is quite different compared with phase lag obtained with glass cell (see Fig. 3).

B. Frequency Scanning: Transmission or Reflection

Let us consider the previous studied configurations, namely, the trilayer material. In order to perform a frequency scanning, a decade $f \in [0.05; 0.5]$ is covered. The phase lag evolution at the center of the heated surface ($z = 0$ [m]) in reflection configuration and in transmission configuration ($z = 2.10^{-3}$ [m]) (relative to that obtained at $f = 0.05$ [Hz]) is plotted versus frequency.

In Fig. 7, a mix cell is studied (stainless steel + water + glass). It has been previously shown that transmission results are similar whatever the heated face is. Then, the following cases are presented.

1) Case E (transmission): heated steel face + water + glass.
2) Case F (reflection): heated steel face + water + glass.
3) Case G (reflection): heated glass face + water + stainless steel.

Considering Figs. 6 and 7, one can note that the phase lag is much more significant in transmission configurations than in reflection configurations and that a glass cell would allow one to obtain more signal than a stainless steel cell. Moreover, a mix cell can be used in transmission.

C. Effect of Liquid Thermal Properties

The previous analyses are performed according to numerical simulations considering that a cell is full of water. In order to extend the previous analysis to other kinds of liquids, let us consider the liquid thermal properties in Table I (see [13] and [19]).

In the following, phase lag is investigated in the previous studied configurations for each liquid in order to study spatial scanning (S) and frequency scanning (F), and in transmission (T) or reflection (R). Comparisons with water are performed considering the results shown in Figs. 2–7.

Considering the maximum of relative differences given in Table II and the results shown in Figs. 2–7, the following partial conclusions are valid for several kinds of liquids (water, paraffin oil, ethanol, and blood).

D. Partial Conclusion

This feasibility study has ensured that a spatial scanning analysis (Figs. 2–5) or a frequency scanning analysis (Figs. 6 and 7) could provide enough informative signals to test trilayer cells containing the unknown material. The insulating cell made

TABLE I
SOME LIQUID THERMAL PROPERTIES

	thermal conductivity $\left[\mathrm{W.m^{-1}.K^{-1}}\right]$	volumetric heat capacity $\left[\mathrm{J.m^{-3}.K^{-1}}\right]$
water	$\lambda = 0.6$	$C = 4.2\ 10^6$
paraffin oil	$\lambda = 0.15$	$C = 1.7\ 10^6$
ethanol	$\lambda = 0.26$	$C = 2.6\ 10^6$
blood	$\lambda = 0.49$	$C = 4.4\ 10^6$

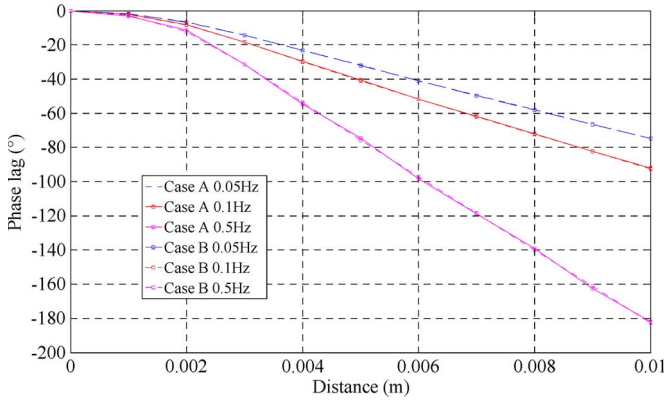

Fig. 4. Simulated phase lag in transmission for a mix cell at different frequencies considering a spatial scanning.

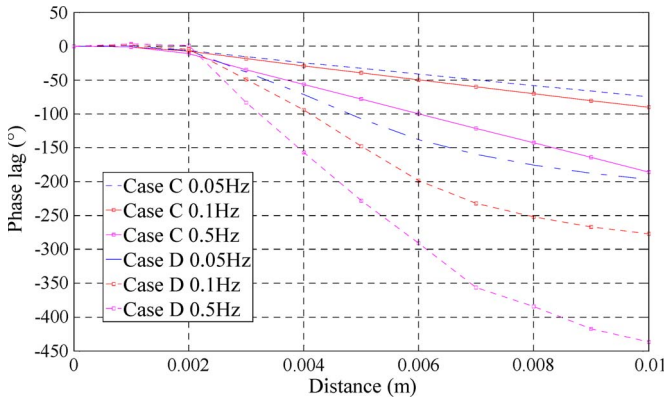

Fig. 5. Simulated phase lag in reflection for a mix cell at different frequencies considering a spatial scanning.

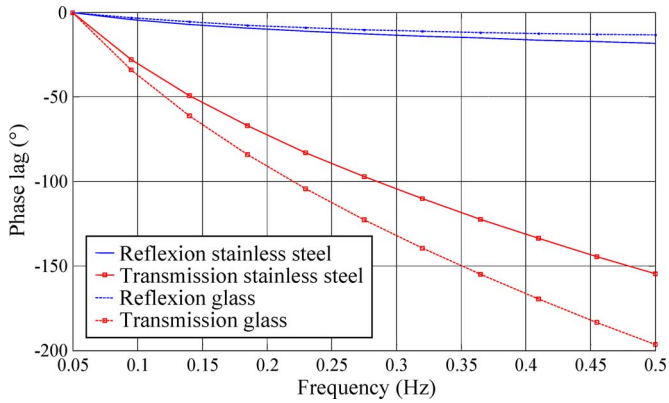

Fig. 6. Simulated phase lag in reflection and in transmission for a stainless steel sample and a glass sample considering a frequency scanning.

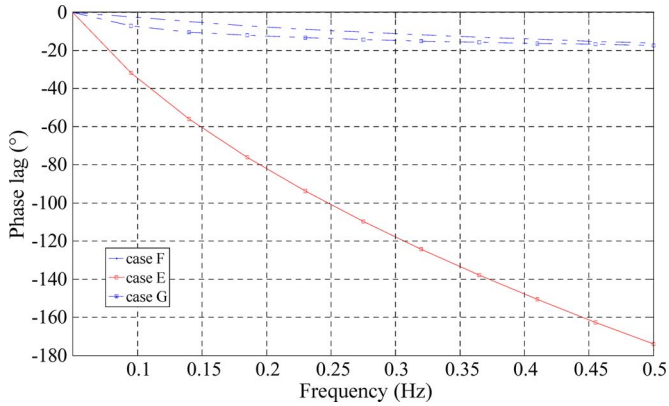

Fig. 7. Simulated phase lag in reflection and in transmission for a mix cell considering a frequency scanning.

of glass would be more appropriate than the conductive cell made of stainless steel, and only analysis in transmission is possible in frequency scanning. A mix cell (glass face and steel face) can be used and provide different phase lags (than steel cell or glass cell) in frequency scanning (only in transmission) or in spatial scanning (in reflection, phase lag is greater if the glass face is heated). In the following paragraph, an optimal configuration will be proposed.

IV. Optimal Design for the Identification Purpose

In order to estimate the effect of the parameter uncertainties, it is essential to achieve a sensitivity analysis. While the evolution of the process state is obtained by solving the forward problem, the sensitivity analysis is performed by computing the sensitivity functions which are a solution of the sensitivity problem derived from the direct problem. A sensitivity study of an observable [in this case, the observed phase lag $\varphi(X) = \arg(\tilde{\theta}(X))$] on the n model parameters $\beta = [\beta_1, \beta_2, \ldots, \beta_n]$ allows either to reduce the forward model or to discuss the possibility of an accurate physical parameter identification. Sensitivity functions are defined as the absolute variation of the observable induced by an absolute variation of the considered parameter. In order to compare these coefficients with each other, the reduced sensitivity functions of $\varphi(X) = \arg(\tilde{\theta}(X))$ versus parameter β_i are defined by

$$X^*_{\beta_i} = \beta_i \frac{\partial \varphi(\beta)}{\partial \beta_i}. \tag{5}$$

It is important to notice that this reduced sensitivity function contains not only the amplitude variation but also its sign. The considered parameter identification will be all the more easier and accurate since this function amplitude is high. In fact, for a given application, if the reduced sensitivity function versus an

TABLE II
COMPARISON WITH WATER: MAXIMUM OF THE RELATIVE DIFFERENCE

cell	(T)	(R)	(S)	(F)	previous figure	paraffin oil	ethanol	blood
steel	x		x		figure 2	10%	6%	1%
steel		x	x		figure 3	14%	12%	4%
steel	x			x	figure 6	19%	12%	9%
steel		x		x	figure 6	4%	3%	2%
glass	x		x		figure 2	20%	16%	6%
glass		x	x		figure 3	33%	22%	14%
glass	x			x	figure 6	24%	18%	10%
glass		x		x	figure 6	146%	100%	20%
mix	x		x		figure 4	10%	9%	3%
mix		x	x		figure 5	22%	14%	8%
mix	x			x	figure 7	18%	14%	9%
mix		x		x	figure 7	40%	34%	15%

unknown parameter is weak on the considered domain (space or frequency domain...), then information on this parameter contained in observable measurements is poor. It comes that if this reduced function is equal to zero, then the considered parameter cannot be identified from this observable. Moreover, if the reduced functions versus two parameters are linearly dependent, it can only be possible to identify a relationship between them. This sensitivity study has to be performed not only for the unknown parameters but also for the known parameters (which are *a priori* known with given uncertainties). Thus, the sensitivity function analysis leads to determine satisfactory conditions in order to accurately identify thermal diffusivity of the unknown liquid. However, it is necessary to consider a nominal state of the system. Three configurations are studied: Unknown liquid is water, and cells are made of glass $\beta_i \in \beta_{\text{glass}} = \{\alpha_{\text{glass}}, \alpha_{\text{water}}, h, e_{\text{glass}}, e_{\text{water}}, r, \omega\}$ or made of stainless steel $\beta_i \in \beta_{\text{steel}} = \{\alpha_{\text{steel}}, \alpha_{\text{water}}, h, e_{\text{steel}}, e_{\text{water}}, r, \omega\}$ or a mix cell $\beta_i \in \beta_{\text{glass}} \cup \beta_{\text{steel}}$.

Considering the partial conclusions drawn up in Section III-C, sensitivity study is limited to frequency scanning in transmission and spatial scanning in both transmission and reflection.

A. Frequency Scanning in Transmission

In Fig. 8 are shown the reduced sensitivity functions for a cell made of stainless steel.

Fig. 8 analysis leads to the following remarks.

1) The reduced sensitivity function of the phase lag to α_{water} is higher than those to α_{steel}, h, e_{steel}, and r.
2) It is quite important to accurately control the periodic excitation frequency $f = \omega/2\pi$ and the internal cell thickness e_{water}.

In Fig. 9 are shown the reduced sensitivity functions for a cell made of glass.

Fig. 9 shows that the sensitivity functions of the phase lag to the glass thickness e_{glass} of the cell and to its thermal diffusivity α_{glass} are not neglectable even if the identification of the thermal diffusivity of water is possible by accurately controlling the periodic excitation frequency $f = \omega/2\pi$ and the internal cell thickness e_{water}. In Fig. 10 are shown the reduced sensitivity functions for a mix cell (glass face is heated), and phase lags are observed on the steel face. Results are in good adequacy with Figs. 8 and 9. Thus, analyzing Figs. 8–10 in the studied configuration, it seems that using a cell made of stainless steel is more relevant than using a cell made of glass or a mix cell.

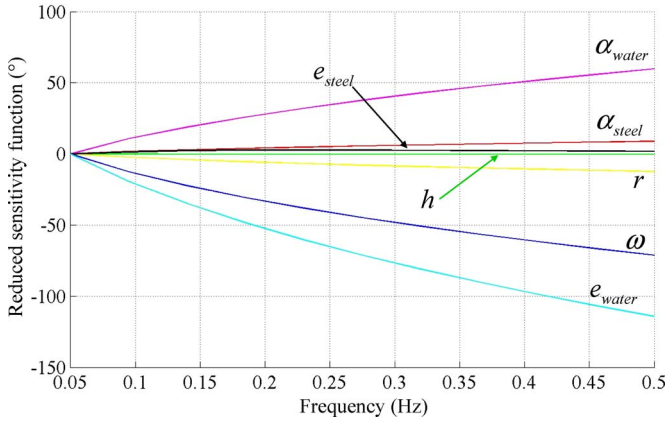

Fig. 8. Reduced sensitivity functions of phase lag to parameters for a stainless steel cell considering a frequency scanning.

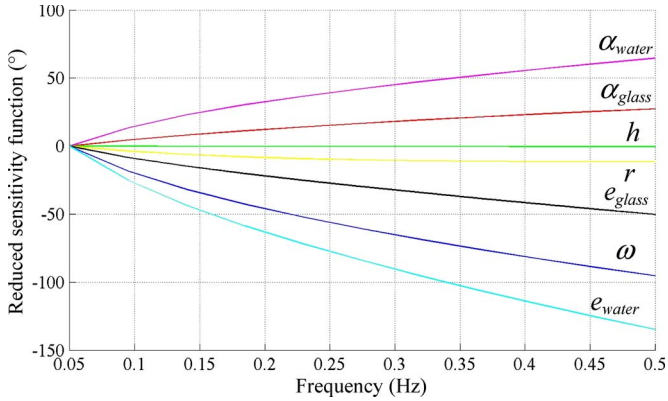

Fig. 9. Reduced sensitivity functions of phase lag to parameters for a glass cell considering a frequency scanning.

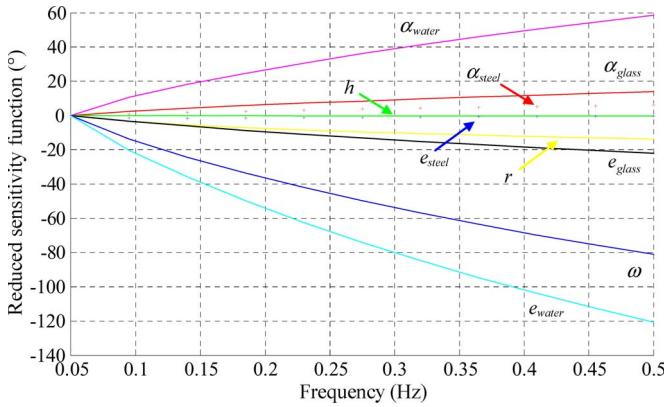

Fig. 10. Reduced sensitivity functions of phase lag to parameters for a mix cell considering a frequency scanning.

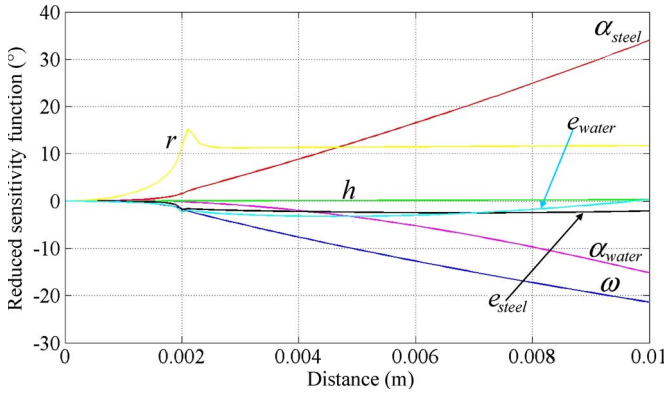

Fig. 11. Reduced sensitivity functions of phase lag to parameters for a stainless steel cell considering a spatial scanning in reflection.

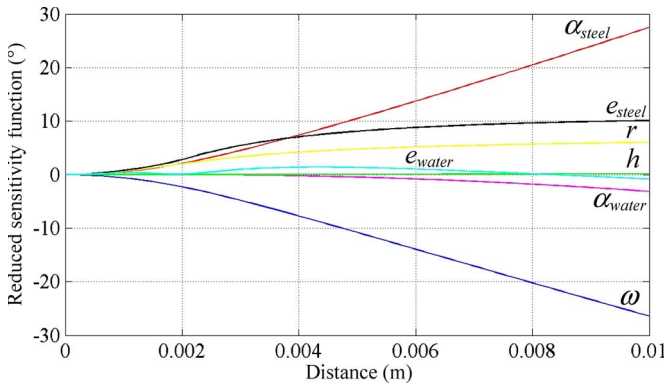

Fig. 12. Reduced sensitivity functions of phase lag to parameters for a stainless steel cell considering a spatial scanning in transmission.

B. Spatial Scanning for a Cell Made of Stainless Steel

For this configuration, the excitation frequency is fixed ($f = 0.05$ Hz). In Figs. 11 and 12, the reduced sensitivity functions of the phase lag to all the parameters are shown versus distance from the center of the nonheated face.

This reduced sensitivity analysis (Figs. 11 and 12) leads to put in evidence that the phase lag obtained by a spatial scanning for a cell made of stainless steel both in transmission and in reflection is sensitive to a large number of parameters. In particular, the reduced sensitivity function to the unknown parameter α_{water} is weak on the considered domain compared to ω, α_{steel}, and r (e_{steel} in transmission). Then, information contained in observable measurements on this parameter is too poor in order to achieve an accurate identification.

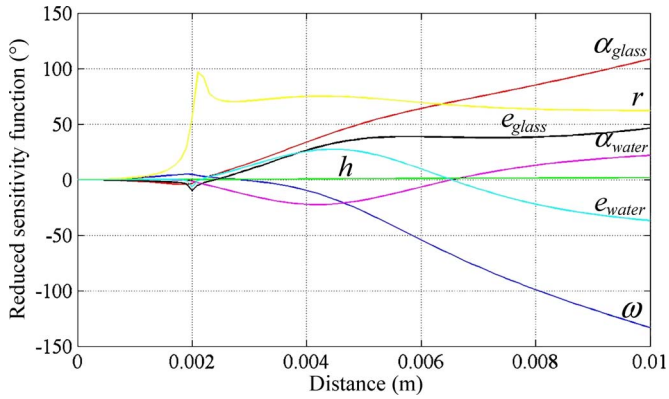

Fig. 13. Reduced sensitivity functions of phase lag to parameters for a glass cell considering a spatial scanning in reflection.

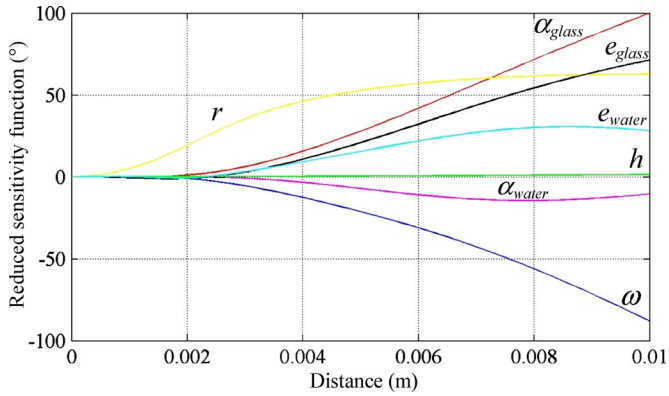

Fig. 14. Reduced sensitivity functions of phase lag to parameters for a glass cell considering a spatial scanning in transmission.

C. Spatial Scanning for a Cell Made of Glass

This reduced sensitivity analysis (Figs. 13 and 14) leads to put in evidence that the phase lag obtained by a spatial scanning for a cell made of glass both in transmission and in reflection is sensitive to a lot of process parameters. In particular, the reduced sensitivity function to the unknown parameter α_{water} is weak on the considered domain compared to ω, α_{glass}, e_{water}, and r. Then, as previously mentioned, information contained in observable measurements on this parameter is too poor to achieve an accurate identification.

D. Spatial Scanning for a Mix Cell

Let us consider the results obtained with a mix cell heated on the glass face (Fig. 15 in transmission and Fig. 16 in reflection).

It is shown in Figs. 15 and 16 that (in transmission as well as in reflection) phase lag sensitivity to the unknown parameter α_{water} is in the same magnitude as that to numerous parameters such as the heating source radius, the steel thermal diffusivity, the excitation frequency, the internal layer thickness (e_{water}), and the observed face thickness (glass face in reflection; steel face in transmission).

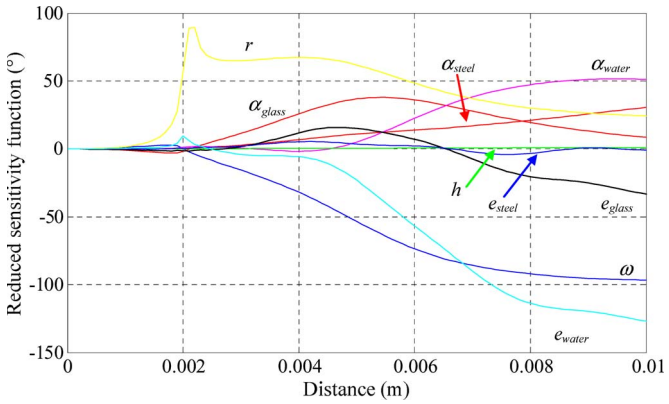

Fig. 15. Reduced sensitivity functions of phase lag to parameters for a mix cell considering a spatial scanning in reflection.

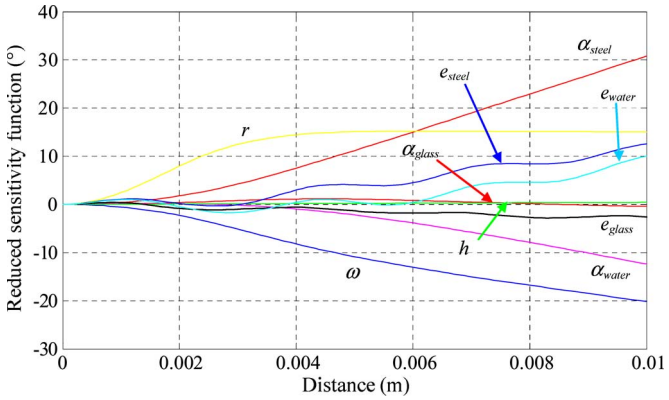

Fig. 16. Reduced sensitivity functions of phase lag to parameters for a mix cell considering a spatial scanning in transmission.

E. Partial Conclusion

The results of the reduced sensitivity analysis have put in evidence that optimal configuration for liquid thermal diffusivity identification is obtained when a steel cell is considered and when a frequency scanning in transmission is performed. In fact, in this experimental configuration, phase lag measurement is sensitive to the unknown thermal parameter but does not dramatically depend on other parameters (assumed to be known with a given accuracy).

V. Numerical Validation Considering Noisy Disturbed Simulated Phase Lag

In the following paragraph, an example of thermal diffusivity identification of a liquid is implemented in the optimal case (cell made of stainless steel and frequency scanning in transmission). Phase lag is defined at the upper face center as the difference between phase lag obtained at a given frequency and phase lag obtained at frequency ($f = 0.05$ Hz). Simulated phase lag is obtained considering frequency range ($f \in [0.05, 0.5]$ Hz) and for the following set of input parameters:

$$\alpha_{\text{steel}} = 1.2\ 10^{-5}\ [\text{m}^2 \cdot \text{s}^{-1}] \quad e_{\text{steel}} = 5\ 10^{-4}\ [\text{m}]$$
$$\alpha_{\text{liq}} = 10^{-6}\ [\text{m}^2 \cdot \text{s}^{-1}] \quad e_{\text{liq}} = 10^{-3}\ [\text{m}]$$
$$r = 2\ 10^{-3}\ [\text{m}] \quad h = 10\ [\text{W} \cdot \text{m}^{-2} \cdot \text{K}^{-1}].$$

A finite-element method is implemented in order to solve the system of partial differential (2) satisfied by complex temperature. A Levenberg–Marquardt numerical algorithm for the resolution of the identification problem has been implemented in order to identify the unknown parameter α_{water}. The following quadratic criterion $J(\alpha)$ describing the difference between measured phase lags $\hat{\varphi}_i$ and simulated phase lags φ_i has to be minimized:

$$J(\alpha) = \sum_{i=1}^{N} \left(\hat{\varphi}_i - \varphi_i(\alpha)\right)^2 \tag{6}$$

where N is the number of experimental frequencies. Identification results considering initial value $\alpha_{\text{liq}} = 10^{-5}$ $[\text{m}^2 \cdot \text{s}^{-1}]$ are shown in Fig. 17. Convergence is achieved in few iterations, and identified thermal diffusivity is $\alpha_{\text{liq}} \approx 10^{-6}$ $[\text{m}^2 \cdot \text{s}^{-1}]$.

In experimental cases, phase lag is noisy and disturbed. Therefore, it is necessary to ensure that the identified thermal diffusivity value remains coherent considering noise [22]. Thus, robustness of this approach is investigated while a realistic noise is generated on simulated phase lag (a Gaussian random generator is used $N(0, \sigma)$). In Table III, relative error compared to $\alpha_{\text{liq}} = 10^{-6}$ $[\text{m}^2 \cdot \text{s}^{-1}]$ is indicated for several noise levels.

In Fig. 18, identification results are shown in the most disadvantageous case: disturbances law $N(0, 10)$.

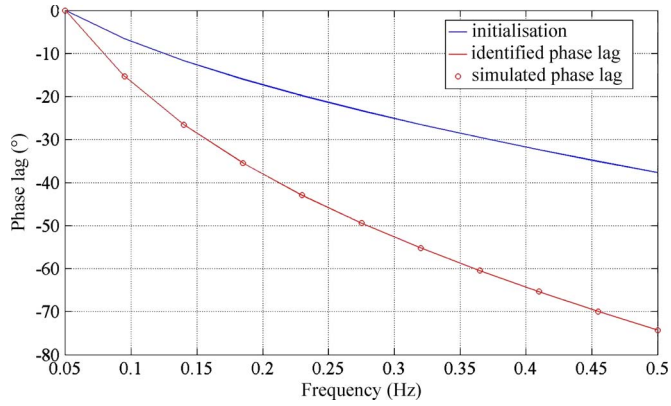

Fig. 17. Example of identification results.

TABLE III
Error Estimation

Standard deviation	$\sigma = 1°$	$\sigma = 5°$	$\sigma = 10°$
Relative error %	1.88	2.66	4.44

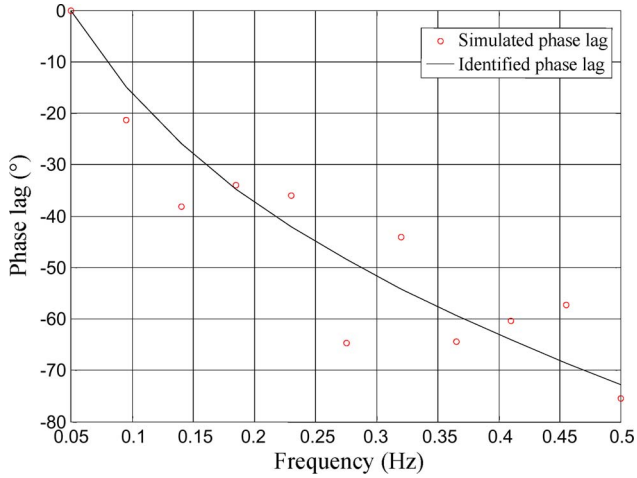

Fig. 18. Identification results considering disturbed phase lags.

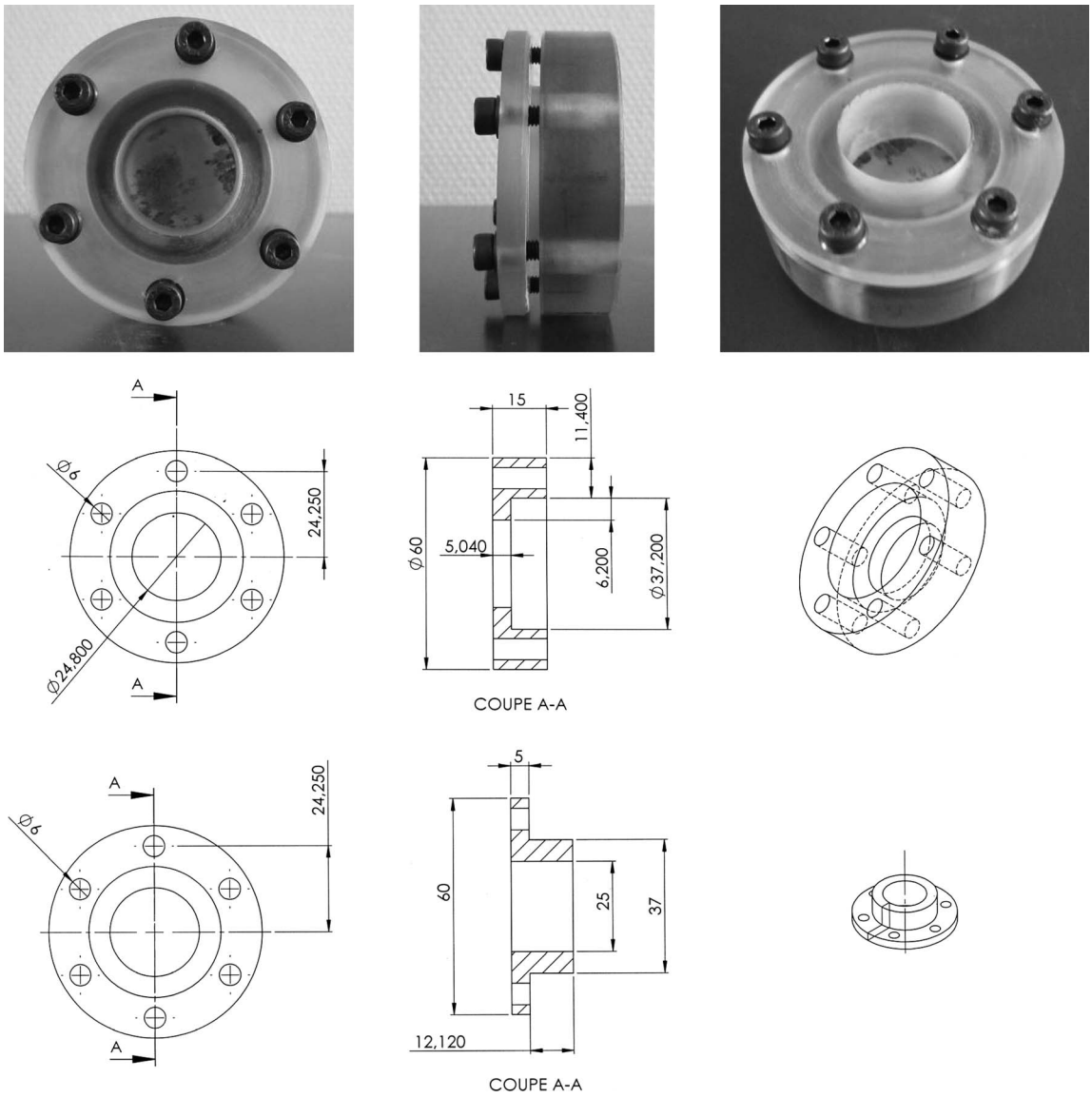

Fig. 19. Proposed experimental steel cell (dimensions are in millimeters).

Results are quite satisfactory because, even if noise is overestimated, convergence is fast (seven iterations) and error on identified parameter is less than 5%. Considering the previous sections, an experimental bench dedicated to the identification of the thermal diffusivity of an unknown liquid has been developed. Early results are shown in the following section.

VI. Experimental Validation

The following elements have been selected for experimental implementation. Heating flux is provided by a halogen lamp (power adjustable, maximum of 1500 W). A Köhler optical assembly is proposed in order to obtain a uniform spatial distribution on a disk (radius adjustable by a diaphragm) of the heat flux on the lower face of the sample. To heat the sample by a periodic way, two different procedures are possible: At low frequency (period longer than 5 s), the power of the lamp is controlled by a mechanical power switch, while at higher frequency (period less than half a second), an optical chopper with adjustable and controlled speed is used (the lamp being switched on continuously). These choices allow one to overcome the delay induced by the heating of the filament which may not be reproducible at high frequency. Temperature observations are obtained on the upper face of the sample by an infrared camera. The spatial distribution of the temperature on the sample recorded by the IR camera is representative of the material's nature and could inform about defects in the trilayer sample (bubbles inside the liquid, for example). The signal processing allows one to extract the amplitude of the signal and the phase lag between periodic input and thermal response of the material, even if the noise level is high. Spatial distributions analysis is performed in order to define the maximum temperature, the excitation frequency, and the distance between IR camera and the observed face. A 200 $\times$ 200 pixels square area is usually considered, and it is necessary to record at least 50 IR pictures during more than 10 periods (in steady state) in order to calculate modulus and phase lag. Thus, considering a period of the heating excitation lower than 1 s, an IR camera allowing a data acquisition frequency of up to 50 Hz is required.

TABLE IV
EXPERIMENTAL RESULTS: IDENTIFIED THERMAL DIFFUSIVITY ($m^{-2} \cdot s^{-1}$)

	Reference value	Identified	Relative error
water	$\alpha = 1.4\ 10^{-7}$	$\alpha \approx 1.52\ 10^{-7}$	$\approx 9\%$
ethanol	$\alpha = 10^{-7}$	$\alpha \approx 0.94\ 10^{-7}$	$\approx 6\%$

The proposed cell is shown in Fig. 19. The resulting cell structure defines a cavity—which thickness is accurately known—to contain the liquid. Once the liquid is in, the cell can be held horizontally or vertically. Care should be given to viscous liquid to avoid air bubble or thin air layer. Considering a vertical configuration, it is well known that convective exchanges vary along the height of the sample. Thus, IR images will have to be carefully analyzed before taking into account a possible simplifying assumption in axisymmetric geometry.

The experimental device and the whole approach are validated owing to several experimentations using liquids considered as reference (water and ethanol). Frequency scanning in transmission is performed for steel cell filled with investigated liquid. In the following table, the average identified thermal diffusivity is given (considering several experimentations and phase lag measurements).

Considering the relative error given in Table IV, both the experimental bench and the identification methodology are validated for further investigations.

VII. CONCLUDING REMARKS

In this paper, identification of the thermal diffusivity of a liquid has been studied under constraint of a weak heating flux. Indeed, for fluids, a too high temperature irrevocably alters the material. One can mention the example of blood thermal properties which are input parameters of numerous mathematical models in life science and which are very difficult to find in literature with great accuracy. Considering this constraint, a methodology based on the analysis of thermal waves generated by a periodic heating has been proposed. In this context, an optimal design has been investigated owing to a sensitivity study based on a mathematical model describing heat transfer (module and phase lag of temperature oscillations) in a 3-D geometry by a system of partial differential equations. A minimization procedure has been implemented, and the effect of measurement noise has been analyzed. Thus, an experimental device has been developed and presented (some technical aspects have been briefly developed). Several liquids (considered as references) have been investigated, and the results obtained for thermal characterization validate the proposed approach.

In a further step, an experimental campaign will be conducted on biological materials whom thermophysical parameters are not accurately defined in temperature (blood . . .). Then, considering correct input parameters, a predictive mathematical model for heat transfer simulation in human skin can be developed.

ACKNOWLEDGMENT

The authors would like to thank their colleagues of the Principal Solar Furnace of the Ministry of Defense (in Font Romeu France): A scientific collaboration around the theme addressed in this paper has been fruitful for a decade.

REFERENCES

[1] J. Opsal, A. Rosencwaig, and D. L. Willenborg, "Thermal-wave detection and thin-film thichness measurements with laser-beam deflection," *Appl. Opt.*, vol. 22, no. 20, pp. 3169–3176, Oct. 1983.
[2] A. Salazar, A. Sanchez-Lavega, and J. M. Terron, "Effective thermal diffusivity of layered materials measured by modulated photothermal techniques," *J. Appl. Phys.*, vol. 84, no. 6, pp. 3031–3041, Sep. 1998.
[3] W. Czarnetzki and W. Roetzel, "Temperature oscillation techniques for simultaneous measurement of thermal diffusivity and conductivity," *Int. J. Thermophys.*, vol. 16, no. 2, pp. 413–422, Mar. 1995.
[4] Determination of Thermal Conductivity and Thermal Diffusivity, Part 3: Temperature Wave Analysis Method, ISO Std. 22007-3, 2008.
[5] L. Perez and L. Autrique, "Robust determination of thermal diffusivity values from periodic heating data," *Inverse Probl.*, vol. 25, no. 4, p. 045011, Apr. 2009.
[6] L. Autrique, L. Perez, and J. J. Serra, "Finite element modelling for microscale thermal investigations using photothermal microscopy data inversion," *Meas. Sci. Technol.*, vol. 18, no. 1, pp. 1–11, Jan. 2007.
[7] L. Autrique, L. Perez, and E. Scheer, "On the use of periodic photothermal methods for materials diagnosis," *Sens. Actuators B, Chem.*, vol. 135, no. 2, pp. 478–487, Jan. 2009.
[8] S. Pittois, M. Chirtoc, C. Glorieux, W. Van den Bril, and J. Thoen, "Direct determination of thermal conductivity of solids and liquids at very low frequencies using the photopyroelectric method," *Anal. Sci.*, vol. 17, pp. S110–S113, 2001.
[9] D. Dadarlat, C. Neamtu, E. Surducan, A. Hadj Sahraoui, S. Longuemart, and D. Bicanic, "Accurate photopyroelectric measurements of thermal diffusivity of (semi)liquids," *Instrum. Sci. Technol.*, vol. 30, no. 4, pp. 387–396, 2002.
[10] J. A. Balderas-López and A. Mandelis, "Self-consistent photothermal techniques: Application for measuring thermal diffusivity in vegetable oils," *Rev. Sci. Instrum.*, vol. 74, no. 1, pp. 700–702, Jan. 2003.
[11] A. Matvienko and A. Mandelis, "Quantitative one-dimensional thermal-wave cavity measurements of fluid thermophysical properties through equivalence studies with three-dimensional geometries," *Rev. Sci. Instrum.*, vol. 77, no. 6, pp. 064906-1–064906-9, Jun. 2006.
[12] S. Delenclos, D. Dadarlat, N. Houriez, S. Longuemart, C. Kolinsky, and A. Hadj Sahraoui, "On the accurate determination of thermal diffusivity of liquids by using the photopyroelectric thickness scanning method," *Rev. Sci. Instrum.*, vol. 78, no. 2, pp. 024902-1–024902-5, Feb. 2007.
[13] P. C. Menon, R. N. Rajesh, and C. Glorieux, "High accuracy, self-calibrating photopyroelectric device for the absolute determination of thermal conductivity and thermal effusivity of liquids," *Rev. Sci. Instrum.*, vol. 80, no. 5, pp. 054904-1–054904-9, May 2009.
[14] D. Dardalat and M. N. Pop, "New front photopyroelectric methodology based on thickness scanning procedure for measuring the thermal parameters of thin solids," *Meas. Sci. Technol.*, vol. 21, no. 10, p. 105 701, Oct. 2010.
[15] T. A. Balasubramaniam and H. F. Bowman, "Thermal conductivity and thermal diffusivity of biomaterials: A simultaneous measurement technique," *J. Biomech. Eng.*, vol. 99, no. 3, pp. 148–154, Aug. 1977.
[16] A. Dumas and G. S. Barozzi, "Laminar heat transfer to blood flowing in a circular duct," *Int. J. Heat Mass Transf.*, vol. 27, no. 3, pp. 391–398, Mar. 1984.
[17] E. Ponder, "The coefficient of thermal conductivity of blood and of various tissues," *J. Gen. Physiol.*, vol. 45, no. 3, pp. 545–551, Jan. 1962.
[18] A. N. Takata, "Development of criterion for skin burns," *Aerosp. Med.*, vol. 45, no. 6, pp. 634–637, 1974.
[19] T. Peng, D. P. O'Neill, and S. J. Payne, "A two-equation coupled system for determination of liver tissue temperature during thermal ablation," *Int. J. Heat Mass Transf.*, vol. 54, no. 9/10, pp. 2100–2109, Apr. 2011.
[20] L. Autrique and C. Lormel, "Numerical design of experiment for sensitivity analysis—Application to skin burn injury prediction," *IEEE Trans. Biomed. Eng.*, vol. 55, no. 4, pp. 1279–1290, Apr. 2008.
[21] C. Lormel, L. Autrique, and B. Claudet, "Mathematical modelling of skin behavior during a laser radiation exposure," in *Proc. 2nd Eur. Survivability Workshop March*, Noordwijk, The Netherlands, 2004, [CD-ROM].
[22] E. Walter and L. Pronzato, *Identification of Parametric Models From Experimental Datas*. Berlin, Germany: Springer-Verlag, 1997.

Laetitia Perez received the Postgraduate degree (DEA) in process engineering from the University of Perpignan, Perpignan, France, in 2000 and the Ph.D. degree from the Ecole Nationale Supérieure des Arts et Métiers, Paris, France, in 2003.

From 2004 to 2006, she had a temporary research monitoring position with the E.H.F Department (Expertise Hauts Flux), D.G.A. (Weaponry Department of French Ministry of Defence) Font Romeu, France. In 2006, she joined the Laboratoire de Thermocinétique de Nantes, Nantes, France, where she is currently an Associate Professor. Her research interests include the modeling of thermal process, the experimental bench development, and the resolution of inverse heat conduction problems.

Laurent Autrique received the Postgraduate degree (DEA) in process control and the Ph.D. degree from the Ecole Centrale, Nantes, France, in 1992 and 1995, respectively.

He was a Research Scientist with the PROMES Research Institute (C.N.R.S. Perpignan, Perpignan, France) until 2002. From 2002 to 2007, he was with the E.H.F. Department (Expertise Hauts Flux), D.G.A. (Weaponry Department of French Ministry of Defence) Font Romeu, France. He is currently a Professor with the Laboratoire d'Ingénierie des Systèmes Automatisés (LISA-ISTIA, University of Angers, Angers, France). His research works are devoted to parametric identification, inverse problems, process analysis, and systems control theory. His main publications are focused on nonlinear partial differential equation systems describing state evolution of complex thermal processes.